ДОПОВІДІ
НАЦІОНАЛЬНОЇ
АКАДЕМІЇ НАУК
УКРАЇНИ

НАУКИ ПРО ЗЕМЛЮ
GEOSCIENCES

https://doi.org/10.15407/dopovidi2023.03.049
UDC 550.4 (477); 551.21:551.24

G.V. Artemenko[1], https://orcid.org/0000-0002-4528-6853
L.V. Shumlyanskyy[1, 2], https://orcid.org/0000-0002-6775-4419
L.S. Dovbysh[1]

[1] M.P. Semenenko Institute of Geochemistry, Mineralogy and Ore Formation of the NAS of Ukraine, Kyiv
[2] Curtin University, School of Earth and Planetary Sciences, Perth, Australia
E-mail: regulgeo@gmail.com, leonid.shumlyanskyy@curtin.edu.au,

The age of detrital zircon from metasedimentary rocks of the Ternuvate strata (West Azov block of the Ukrainian Shield)

Presented by Academician of the NAS of Ukraine O.M. Ponomarenko

The Ternuvate strata comprise metamorphic rocks that make up the Haichur arcuate structure, which is about 72 km long. Its western part lies within the Andriivka fault zone, which separates the Vovcha and Huliaipole blocks, while the eastern part is located within the Ternuvate fault zone, traced on the Remivka block. The rocks composing the Haichur structure have irregular and laterally variable composition, changeable thickness, and exhibit dynamometamorphic structures of boudinage and schistosity. The upper part of the Ternuvate strata mainly consists of metasedimentary rocks, including gneisses, biotite schists, garnet-biotite, magnetite-amphibole, and feldspar quartzites. The lower part comprises volcanogenic rocks such as amphibolites, metaultrabasites, and biotite-amphibole gneisses. Using the LA-ICP-MS method, 38 zircon crystals from muscovite-biotite gneisses in the upper part of the Ternuvate strata were analyzed. Based on the geochemical data, these zircons are metamorphosed graywackes. The zircon crystals belong to several age populations (3.65-3.45 and 3.3-2.95 Ga), corresponding to the major stages of Archean crust formation in the West Azov domain, including the formation of the oldest basement and granite-greenstone complexes of the Paleoarchean and Mesoarchean ages. Identical populations of detrital zircon were found in the early Precambrian metaterrigenous rocks of the Krutobalka Formation in the Sorokyne greenstone structure. The correspondence between the Paleoarchean crust (3.45-3.65 Ga) of the West Azov block of the Ukrainian Shield and the Kursk-Besedine granulite-gneiss area of the Kursk Magnetic Anomaly block is evident, while the Paleoarchean and Mesoarchean complexes (2.9-3.3 Ga) correspond to the Mykhailivka and Orel-Tim granite-greenstone area of the Kursk Magnetic Anomaly block. The Archean complexes of Sarmatia are of the same age as similar formations in the Kaapvaal craton in South Africa, Bastar craton in India, North China Craton, Slave craton in Canada, and others, which formed during the Eoarchaean.

Keywords: *Haichur structure, Ternuvate sequence, muscovite-biotite gneiss, Huliaipole block, Vovcha block, Remivka block, zircon, U-Pb age, metasedimentary rocks.*

Citation: Artemenko G.V., Shumlyanskyy L.V., Dovbysh L.S. The age of detrite zircon from metasedimentary rocks of the Ternuvate strata (West Azov block of the Ukrainian Shield). *Dopov. Nac. akad. nauk Ukr.* 2023. No 3. P. 49—59. https://doi.org/10.15407/dopovidi2023.03.049

Introduction. The Haichur arcuate structure is a complex trough-shaped structure that extends for approximately 72 km, with a monoclinal structure present in its southern part (Fig. 1) [1]. Its western part is located within the Andriivka fault zone, which separates the Vovcha and Huliaipole blocks, while the eastern part occurs in the Ternuvate fault zone, traced on the Remivka block. The metamorphic rocks that comprise the Haichur structure exhibit irregular and laterally variable composition and changing thickness. They display dynamometamorphic structures, including boudinage and schistosity. The Haichur structure consists of metavolcanogenic and metassedimentary rocks, as well as granitoids that have been strongly affected by dislocation metamorphism, and rocks from the old basement that have been displaced due to tectonic processes. The metamorphosed volcanogenic and sedimentary rocks within the Haichur structure belong to the Ternuvate strata, which are divided into two formations [2]. The upper formation, with a thickness of up to 800 m, primarily consists of biotite, muscovite-biotite, garnet-biotite, sillimanite-garnet, locally with cordierite, graphite, biotite-garnet, magnetite-tremolite-garnet gneisses and schists, magnetite-amphibole, feldspar, and amphibole-magnetite quartzites. In the eastern part of the structure, there are layers of amphibole-magnetite quartzites that extend for 0.5—1.0 km [1].

The lower formation, with a thickness of up to 350 m, consists of amphibolites, metaultrabasites, and amphibole-biotite gneiss. The Ternuvate strata reaches its maximum thickness of 1.0 km on the eastern flank of the Haichur structure, while the minimum thickness of about 100 m is observed on its western flank. Paleoproterozoic granites dated at 2.2 Ga cut through the metamorphic rocks of the Ternuvate strata [3]. The Haichur structure is considered by the authors [1, 2] as a greenstone structure similar to the Kosyvtseve greenstone belt, with the upper terrigenous section of the Haichur structure having escaped denudation. On the other hand, other authors [4] suggest that the lower part of the Ternuvate strata consists of rocks from the West Azov Group, while the upper part belongs to the Central Azov Group.

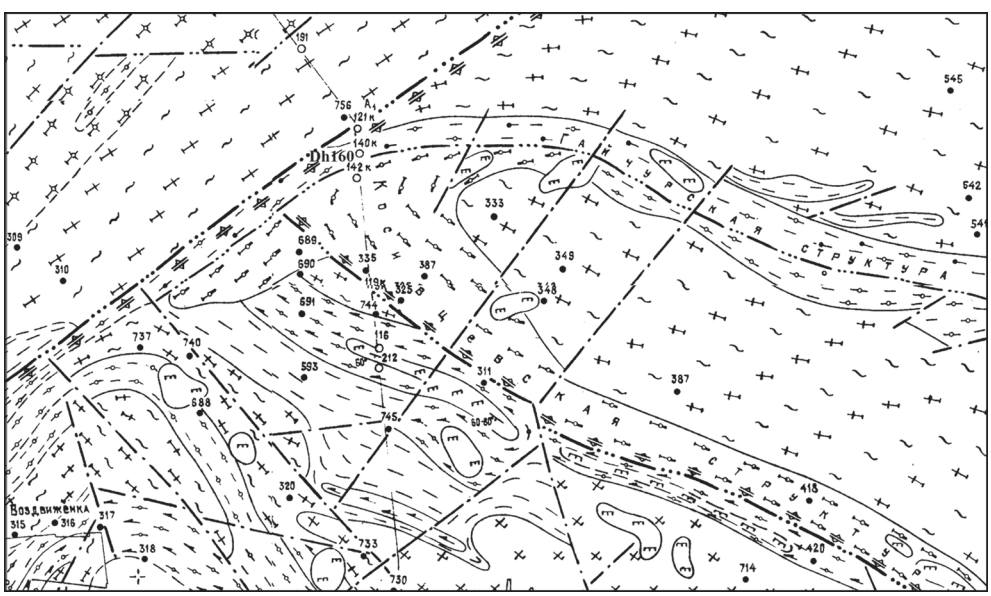

Fig. 1. A schematic geological map of the junction zone of the Huliaipole, Vovcha and Remivka blocks [1], with changes and additions

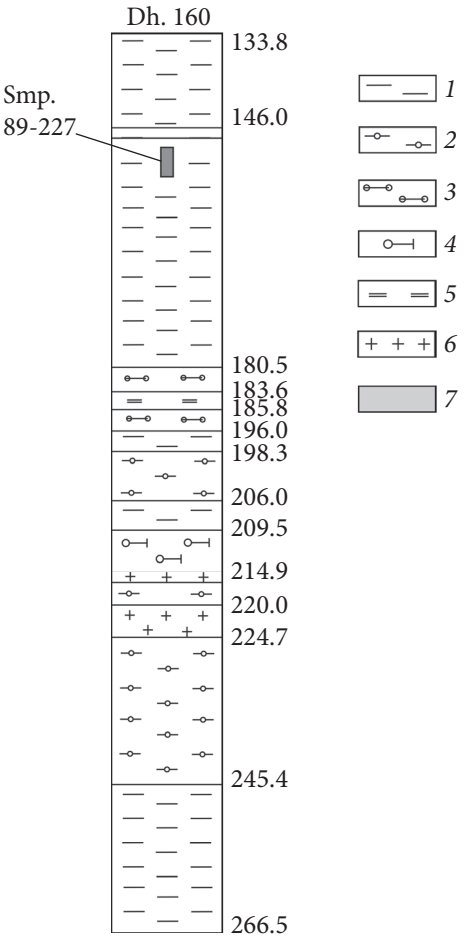

Fig. 2. Schematic log of the borehole No. 160 after [7]: *1* — biotite and two-mica plagioclase gneiss; *2* — two-mica gneiss; *3* — two-mica sillimanite-bearing gneiss; *4* — sillimanite-garnet-biotite plagioclase gneiss; *5* — quartzite; *6* — biotite granite; *7* — sampling interval

Research Objectives. The research objectives were focused on reconstructing the genesis and determining the age of formation of the volcanogenic sedimentary rocks within the Ternuvate strata. Due to the strong tectonic overprint, establishing the genesis of the gneisses and schists within the Ternuvate strata is challenging. To determine their initial nature, the diagrams of A.A. Predovskyi (FAK) [5] and Al_2O_3 — (K_2O+Na_2O) [6] were utilized. Zircon from the biotite gneisses of the Ternuvate strata was dated using the LA-ICP-MS method (sample 89-227, borehole 160, depth 149.8-154.5 m) (Fig. 2).

Research methods. The research methods involved extracting zircon from the rock using a shaking table, heavy liquids, and a magnetic separator to obtain a heavy non-magnetic fraction. Zircons were then hand-picked under a binocular microscope. Zircon morphology was studied using an optical microscope, and the internal structure was documented using cathodoluminescence. U-Pb isotopic data were collected using laser ablation inductively coupled plasma mass spectrometry (LA-ICP-MS) at the GeoHistory Facility, John de Laeter Centre, Curtin University. Zircon standard OG1 (3465 ± 0.6 Ma [8]; all uncertainties at 2σ) was used as the primary reference material, and secondary standards GJ-1 (601.2 ± 0.4 Ma [9]), and Plešovice (337.13 ± 0.37 Ma [10]) were analyzed for comparison. The secondary standards provided weighted mean $^{207}Pb/^{206}Pb$ ages and $^{238}U/^{206}Pb$ ages within the uncertainty of the recommended values. The time-resolved mass spectra were reduced using Iolite 3.7™ [11] and references therein, with final ages calculated using Isoplot. Silicate rock analyses were carried out at the IGMOF of the NAS of Ukraine, Kyiv.

Characteristics of the studied muscovite-biotite gneiss of the Ternuvate strata. The studied muscovite-biotite gneiss from the Ternuvate strata was recovered from borehole 160, located in the northernmost part of the Haichur arcuate structure (see Figs 1, 2). Beneath the weathering crust, within the depth interval of 133.8-180.5 m, muscovite-bearing biotite gneiss was retrieved. The gneiss exhibits indistinct banding, resulting from the alternation of biotite-rich gneiss with relatively leucocratic (biotite below 10 %) gneiss variety. Feldspar is occasionally observed as porphyroblasts, ranging in size up to 5 mm, or as lenses up to 5×6 mm. Biotite flakes vary in size from 0.5×1.0 mm to 3×5 mm. At different intervals, biotite forms clusters, giving the rocks a spotted structure. The gneisses are intruded by veins of aplite granite, which can reach up to 2 cm in thickness.

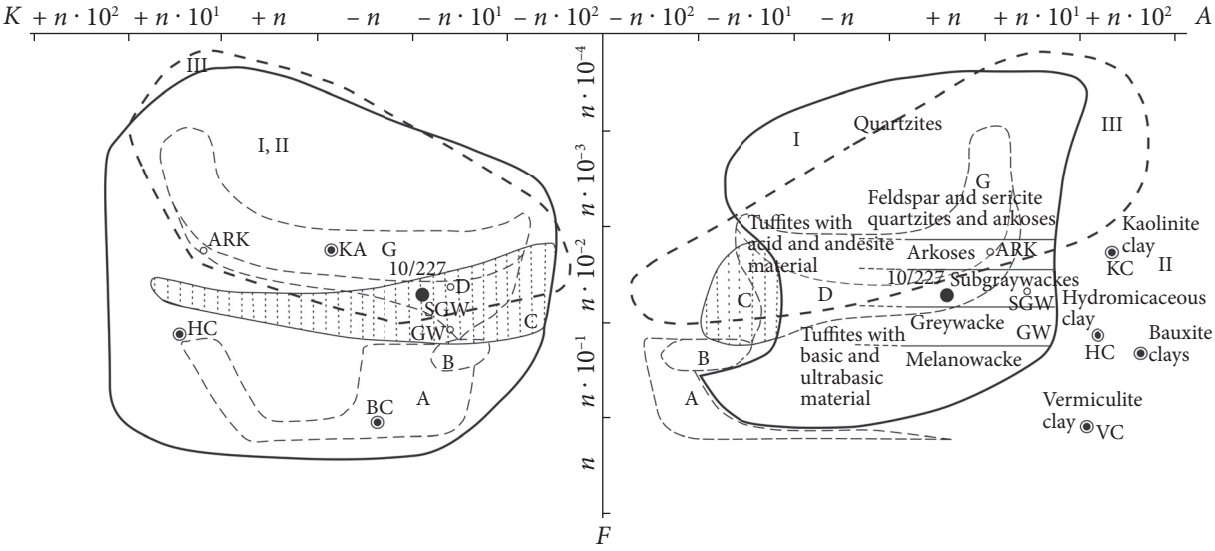

Fig. 3. The FAK diagram [5] is used for the reconstruction of the primary composition of metamorphosed aluminosilicate igneous and sedimentary rocks. Fields of sedimentary, volcanogenic-sedimentary and mixed rocks: I — sedimentary and mixed rocks; II — pelites; III — chemogenic silicites. A — ultrabasites; B — basites; C — syenites, alkaline syenites and their effusive analogues; D — diorites, plagioclase granites and their effusive analogues; G — granites and their effusive analogues. $F = (FeO+MgO+Fe_2O_3)/SiO_2$; $A = Al_2O_3 - (CaO^*+K_2O+Na_2O)$, where $CaO^* = CaO + CO_2$; $K = K_2O - Na_2O$ (in molar amounts) [5]

A sample (89-227) representing muscovite-biotite gneiss from borehole 160, with a depth of 149.8-154.5 m, was selected for the geochronological studies. It is a light gray, fine-grained, and light-banded rock. The mineral composition (%): plagioclase — 45-60; quartz — 30-35; biotite — 10-12; muscovite — 7; opaque minerals, zircon, and apatite occur in accessory amounts.

This rock has high silica and a low alumina content (SiO_2 — 78.62 %; TiO_2 — 0.38 %; Al_2O_3 — 8.84 %; Fe_2O_3 — 0.71 %; FeO — 2.88 %; MnO — 0.09 %; MgO — 1.94 %; CaO — 2.24 %; Na_2O — 1.66 %; K_2O — 1.40 %; S_{total} — 0.10 %; P_2O_5 — 0.12 %; H_2O — 0.15 %; LOI — 0.96 %; Total — 100.09 %).

In the FAK diagram [5], muscovite-biotite gneiss plots within the field of clastic aluminosilicate sedimentary rocks such as subgraywackes and arkoses. It partially overlaps with the field of felsic igneous rocks of similar composition (Fig. 3). The Al_2O_3 — (K_2O+Na_2O) diagram [6] was used to differentiate subgraywacke from metamorphosed felsic and intermediate igneous rocks. In this diagram, muscovite-biotite gneiss plots within the field of subgraywackes (Fig. 4). Another diagram used to distinguish metaarkose and metarhyolite is the $(Fe_2O_3+FeO+MgO)/SiO_2$ — (Na_2O+K_2O) diagram [6], where muscovite-biotite gneiss plots within the field of metagraywacke (Fig. 5).

Zircon characterization. The zircon fraction from muscovite-biotite gneiss (sample 89-227) consists of several varieties of zircon. The predominant form is elongated prismatic crystals with smooth pyramid facets (60 % of the fraction). The crystals have a length along the L_4 axis ranging from 0.2 to 0.35 mm, with an elongation coefficient of 2.0-3.0. They exhibit a pink color and a matte luster. Some grains contain dark cores. Approximately 30 % of the fraction is

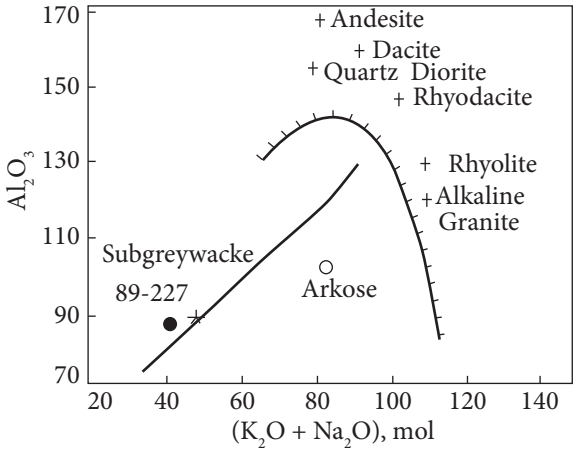

Fig. 4. Diagram Al_2O_3 – $(K_2O + Na_2O)$ (molar amounts) for discrimination of subgraywacke from intermediate and felsic igneous rocks [6]. The trend in the diagram indicates the change of the composition of ordinary sub-graywackes and arkoses with a decreasing amount of quartz

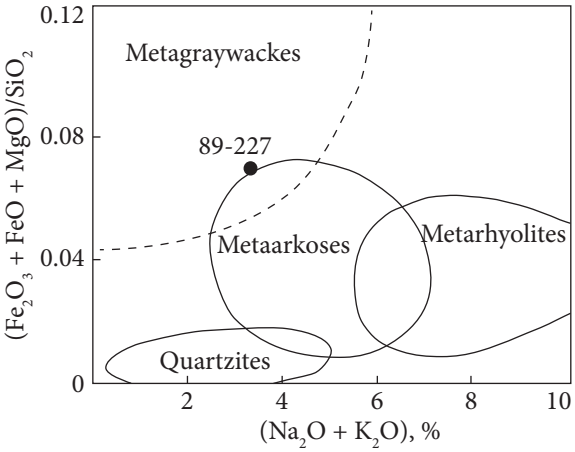

Fig. 5. Diagram $(Fe_2O_3+FeO+MgO)/SiO_2$ – (Na_2O+K_2O) for discrimination of metaarkose and metarhyolite [6]

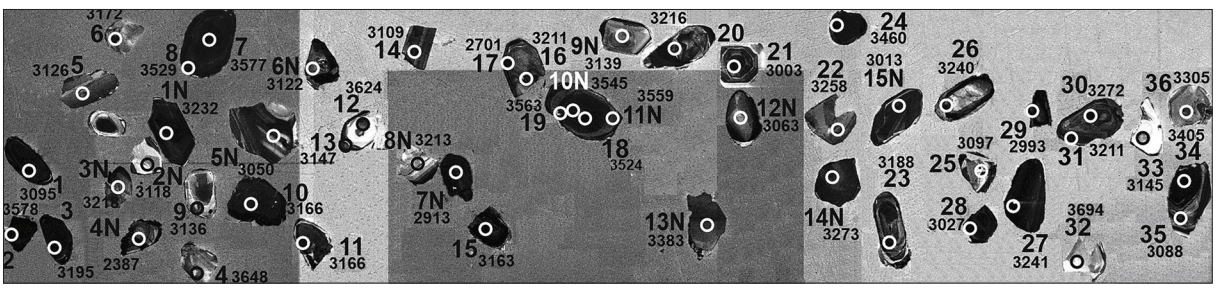

Fig. 6. CL-images of the studied zircon crystals from muscovite-biotite gneiss of the Ternuvate strata (sample 89-227, borehole 160, depth 149.8-154.5 m), with indicated U-Pb analysis numbers (see Table) and $^{207}Pb/^{206}Pb$ isotope age, Ma

composed of pink zircon, which is more transparent and fractured, with a glassy luster and dark cores. A small portion (10 %) of zircon grains is either equant or elongated, with a length along the L_4 axis ranging from 0.15 to 0.35 mm and an elongation coefficient of 1.0-2.5. These crystals also exhibit a pink color, a glassy luster, and transparency. The internal structure of the zircon grains is homogeneous.

The results of geochronological studies of zircon. The LA-ICP-MS method yielded the U-Pb ages for zircon from the muscovite-biotite gneiss in the upper formation of the Ternuvate strata. A total of 38 crystals were dated, with 51 age determinations performed (Table, Figs 6, 7, 8). Among them, 16 dates were highly discordant and were excluded from further consideration. The zircons with discordant ages exhibited elevated levels of uranium, thorium, and lead. The majority of zircon dates (24 crystals) fall within the age range of 3.3-2.95 Ga, while the second most abundant population (9 crystals) is dated at the age of 3.65-3.45 Ga.

Results of U-Pb dating of zircon from muscovite-biotite gneiss (sample 89-227)

# analysis	Concentration, ppm				Isotope ratio							Isotopic age, Ma					
	U	Pb	Th	Th/U	$^{207}Pb/^{235}U$	2σ	$^{206}Pb/^{238}U$	2σ	Rho	$^{207}Pb/^{206}Pb$	2σ	$^{207}Pb/^{235}U$	2σ	$^{206}Pb/^{238}U$	2σ	$^{207}Pb/^{206}Pb$	2σ
1	295	205	295	2,24	19,5400	0,3700	0,6075	0,007	0,37	0,2362	0,007	3095	27	3059	29	3068	19
2*	609	309	609	2,90	26,0000	1,2000	0,5920	0,021	0,94	0,3211	0,021	3578	21	2983	87	3331	46
3	334	217	334	2,34	20,7700	0,6400	0,6120	0,014	0,75	0,2520	0,014	3195	26	3072	56	3133	31
4	61	95	61	1,20	34,7000	1,1000	0,7610	0,017	0,42	0,3380	0,017	3648	47	3643	60	3631	30
5	67	65	67	1,70	21,7500	0,9300	0,6550	0,017	0,32	0,2420	0,017	3126	70	3250	68	3160	41
6	84	100	84	1,46	20,5800	0,7200	0,6080	0,013	0,41	0,2491	0,013	3172	50	3058	50	3119	34
7	311	70	311	7,85	32,9800	0,7400	0,7457	0,009	0,47	0,3213	0,009	3577	24	3590	33	3578	22
8	195	97	195	3,86	32,0500	0,6500	0,7500	0,012	0,45	0,3124	0,012	3529	30	3609	44	3548	20
9	42	49	42	1,44	22,0000	1,0000	0,6730	0,017	0,18	0,2440	0,017	3136	77	3319	68	3178	46
10	179	83	179	3,04	20,5100	0,5400	0,6170	0,011	0,18	0,2464	0,011	3166	42	3094	44	3109	25
11	168	180	168	1,55	21,7700	0,5300	0,6531	0,009	0,20	0,2473	0,009	3166	40	3239	33	3171	24
12	166	96	166	3,18	33,2000	1,1000	0,7350	0,011	0,44	0,3297	0,011	3624	36	3553	42	3590	31
13	111	5	111	102,00	18,9400	0,7300	0,5780	0,013	0,59	0,2457	0,013	3147	47	2936	52	3030	38
14	158	160	158	1,59	20,5100	0,5300	0,6242	0,009	0,43	0,2394	0,009	3109	37	3130	36	3115	25
15*	386	175	386	2,82	14,7000	0,5100	0,4420	0,013	0,74	0,2478	0,013	3163	31	2356	58	2797	34
16	102	53	102	2,97	22,2200	0,6200	0,6430	0,014	0,27	0,2522	0,014	3211	46	3196	55	3193	27
17*	526	73	526	11,45	9,2500	0,3900	0,3760	0,015	0,89	0,1860	0,015	2701	36	2058	72	2382	43
18	309	273	309	2,12	30,5800	0,5800	0,7150	0,009	0,45	0,3115	0,009	3524	24	3480	34	3504	18
19	215	209	215	1,93	32,5700	0,9000	0,7250	0,013	0,73	0,3170	0,013	3563	34	3518	50	3564	29
20	64	28	64	3,37	20,5600	0,7300	0,6000	0,014	0,20	0,2536	0,014	3218	53	3026	57	3118	35
21*	376	164	376	2,12	11,1600	0,3100	0,3685	0,008	0,58	0,2239	0,008	3003	37	2020	38	2533	26
22	70	92	70	1,22	23,1600	0,8300	0,6410	0,015	0,22	0,2630	0,015	3258	63	3188	60	3243	33
23*	219	177	219	1,71	18,2700	0,4400	0,5390	0,012	0,34	0,2500	0,012	3188	39	2775	51	3005	23
24	263	82	263	5,68	28,8200	0,5600	0,7088	0,010	0,49	0,2986	0,010	3460	27	3452	37	3446	19
25*	192	16	192	22,30	16,6200	0,5900	0,5070	0,013	0,59	0,2393	0,013	3097	49	2637	57	2906	34
26	81	58	81	2,82	19,4000	1,0000	0,5680	0,015	0,46	0,2550	0,015	3240	74	2902	64	3068	51

# analysis	Concentration, ppm				Isotope ratio							Isotopic age, Ma					
	U	Pb	Th	Th/U	$^{207}Pb/^{235}U$	2σ	$^{206}Pb/^{238}U$	2σ	Rho	$^{207}Pb/^{206}Pb$	2σ	$^{207}Pb/^{235}U$	2σ	$^{206}Pb/^{238}U$	2σ	$^{207}Pb/^{206}Pb$	2σ
27	265	334	265	1,35	23,3700	0,5900	0,6627	0,009	0,69	0,2579	0,009	3231	27	3276	35	3242	24
28*	248	94	248	4,04	17,8900	0,3400	0,5813	0,007	0,05	0,2269	0,007	3027	31	2953	28	2987	19
29*	254	62	254	5,36	8,9400	0,3500	0,2970	0,012	0,78	0,2226	0,012	2993	38	1676	58	2331	35
30	204	333	204	1,04	24,2900	0,6500	0,6666	0,009	0,40	0,2653	0,009	3272	36	3291	33	3273	26
31	96	196	96	0,81	23,3400	0,6900	0,6740	0,013	0,12	0,2531	0,013	3211	52	3318	50	3236	29
32	38	25	38	3,14	36,2000	1,8000	0,7610	0,022	0,65	0,3480	0,022	3694	54	3639	81	3664	46
33	34	18	34	3,01	20,4000	1,1000	0,6130	0,021	0,30	0,2470	0,021	3135	89	3081	84	3123	52
34	549	460	549	2,37	31,1500	0,7400	0,7310	0,013	0,87	0,3160	0,013	3546	22	3534	49	3525	23
35	117	85	117	2,26	18,6800	0,6500	0,5880	0,012	0,42	0,2345	0,012	3088	48	2984	48	3017	34
36	68	105	68	1,07	24,1100	0,8400	0,6540	0,016	0,24	0,2740	0,016	3305	64	3245	61	3266	35
1N	327	131	327	4,38	24,0162	0,6716	0,6501	0,012	0,39	0,2592	0,012	3263	27	3226	48	3232	41
2N	49	37	49	2,10	21,1017	1,3915	0,6045	0,026	0,18	0,2503	0,026	3125	63	3035	102	3118	111
3N*	89	79	89	1,91	19,6083	0,9806	0,5367	0,016	0,29	0,2583	0,016	3075	48	2764	68	3218	72
4N*	543	58	543	6,27	7,5202	0,2843	0,3382	0,009	0,16	0,1560	0,009	2174	32	1876	44	2387	69
5N	159	141	159	2,01	20,1200	0,8742	0,6040	0,019	0,42	0,2312	0,019	3083	43	3054	81	3050	66
6N	172	141	172	2,08	20,0092	0,8234	0,5846	0,012	0,36	0,2432	0,012	3086	44	2964	51	3122	58
7N*	113	36	113	4,96	18,8645	1,4453	0,6068	0,018	0,37	0,2200	0,018	3005	78	3051	72	2913	113
8N*	308	115	308	2,37	14,7583	0,5440	0,4094	0,015	0,55	0,2574	0,015	2797	39	2207	68	3213	54
9N	112	120	112	1,52	23,2307	0,9270	0,6658	0,016	0,18	0,2440	0,016	3225	39	3286	59	3139	61
10N*	239	197	239	2,34	33,1569	1,1784	0,7386	0,015	0,35	0,3170	0,015	3576	34	3562	55	3545	41
11N*	127	133	127	1,82	34,1972	1,2807	0,7542	0,023	0,42	0,3214	0,023	3605	37	3615	82	3559	56
12N	50	43	50	1,79	21,4051	1,3811	0,6428	0,027	0,39	0,2371	0,027	3137	66	3207	113	3063	105
13N*	83	139	83	1,07	25,7514	1,4202	0,6365	0,019	0,44	0,2881	0,019	3324	58	3169	74	3383	86
14N*	84	125	84	1,21	25,5764	1,3616	0,6791	0,022	0,48	0,2667	0,022	3310	52	3333	83	3273	67
15N	258	248	258	1,62	18,9335	0,6725	0,5974	0,012	0,21	0,2262	0,012	3037	32	3017	47	3013	46

Note. Asterisk (*) indicates discordant analyses that were omitted from Fig. 7 and 8.

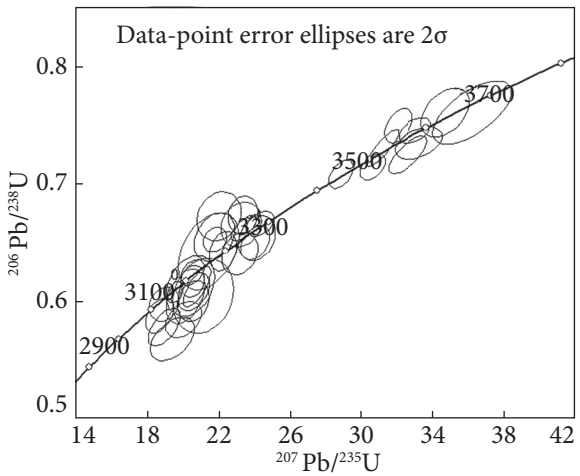

Fig. 7. U-Pb concordia diagram for zircon from muscovite-biotite gneiss of the Ternuvate strata (sample 89-227). Discordant results are omitted

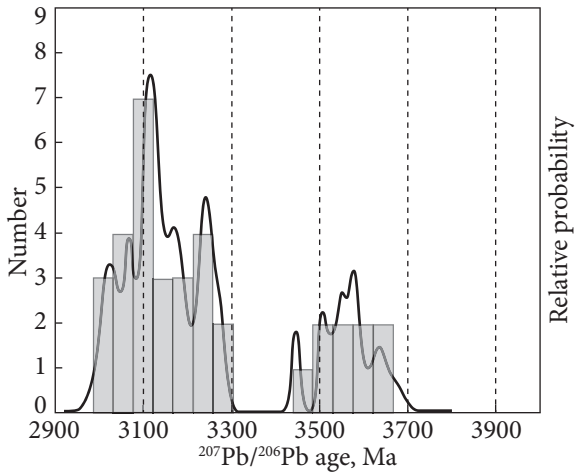

Fig. 8. The $^{207}Pb/^{206}Pb$ age distribution curve for detrital zircon from muscovite-biotite gneiss of the Ternuvate strata (sample 89-227). Only concordant results are plotted

Discussion and conclusions. This geochronological study of the muscovite-biotite gneiss from the upper formation of the Ternuvate strata in the Haichur structure represents the first of its kind. Based on its chemical characteristics, this gneiss is identified as metamorphosed graywacke. Through the application of the LA-ICP-MS method, 38 zircon crystals were dated, resulting in 51 U-Pb age determinations. These zircon populations exhibit ages corresponding to significant stages in the formation of the Archean crust in the West Azov domain. Specifically, the ages range from 3.65-3.45 Ga and 3.3-2.95 Ga, which correspond to the formation of the oldest basement [12—16] and the granite-greenstone complexes of Paleoarchean and Mesoarchean ages, respectively [12, 17]. Similar populations of detrital zircon have been identified in early Precambrian metaterrigenous rocks of the Krutobalka formation in the Soroky greenstone structure [18, 19]. Comparisons between the rock associations of the Ukrainian Shield and the Kursk Magnetic Anomaly provide evidence of a correspondence between the Paleoarchean crust (3.65-3.45 Ga) in the West Azov block and the Kursk-Besedynsk granulite-gneissic area [20, 21]. The Mesoarchean complexes (3.3-2.9 Ga) correspond to the Mykhailivka and Orel-Tim granite-greenstone area of the Kursk Magnetic Anomaly [22, 23]. The Archean complexes in the Sarmatia region exhibit the same ages as similar formations found in the Kaapvaal craton in South Africa [24], Bastar craton in India [25, 26], North China Craton [27], and Slave craton in Canada [28, 29]. These cratons have formed since the Eoarchean period.

REFERENCES

1. Kinshakov, V. N. (1990). Deep geological mapping at a scale 1 : 50000, carried out in 1986-1990. Sheets L-37-1-B, L-37-1-G. Kyiv (in Russian).
2. Isipchuk, K. Yu., Bobrov, O. B., Stepanyuk, L. M. et. al. (2004). Correlative chronostratigraphic chart of the Early Precambrian of the Ukrainian shield (chart and explanatory note). Kyiv: UkrDGRI (in Ukrainian).
3. Artemenko, G. V., Samborska, I. A., Shvaika, I. A., Gogolev, K. I. & Dovbush, T. I. (2018). The stages of Early Proterozoic collision granitoid magmatism and metamorphism on the Azov and Middle-Dnieper megablocks of the Ukrainian Shield. Mineralogical journal, 40, No. 2, pp. 45-62 (in Russian). https://doi.org/10.15407/mineraljournal.40.02.045
4. Pereverzev, S. I. (1989). New data on the age and stratigraphic position of the Osypenkovo Formation (Azov Block). Geologìčnij žurnal, No. 4, pp. 56-64 (in Russian).
5. Predovsky, A. A. (1970). Geochemical reconstruction of the primary composition of metamorphosed volcanogenic-sedimentary formations of the Precambrian. Apatity (in Russian).
6. Predovsky, A. A. (1980). Reconstruction of the conditions of sedimentogenesis and volcanism of the early Precambrian. Leningrad: Nauka (in Russian).
7. Kiktenko, V. F. (1982). Deep geological mapping at a scale smaller than 1 : 200000 within sheets M-37-XXXI, / -37-I, VII (Western Azov region — sheets M-37-133; M-37-134-B; / - 37-1 ; / - 37-2; / -37-13; / - 37-14; / - 37-25-A, B; / - 37-26-A, B). Kyiv (in Russian).
8. Stern, R. A., Bodorkos, S., Kamo, S. L., Hickman, A. H., Corfu, F. (2009). Measurement of SIMS instrumental mass fractionation of Pb isotopes during zircon dating. Geostand. Geoanal. Res., 33, pp. 145-168. https://doi.org/10.1111/j.1751-908X.2009.00023.x
9. Jackson, S. E., Pearson, N. J., Griffin, W. L., Belousova, E. A. (2004). The application of laser ablation-inductively coupled plasma-mass spectrometry to in situ U-Pb zircon geochronology. Chem. Geol., 211, pp. 47-69. https://doi.org/10.1016/j.chemgeo.2004.06.017
10. Sláma, J., Košler, J., Condon, D. J., Crowley, J. L., Gerde, A., Hanchar, J. M., Horstwood, M. S., Morris, G. A., Nasdala, L., Norberg, N., Schaltegger, U., Schoene, B., Tubrett M. N. & Whitehouse, M. J. (2008). Plešovice zircon – a new natural reference material for U-Pb and Hf isotopic microanalysis. Chem. Geol., 249, pp. 1-35. https://doi.org/10.1016/j.chemgeo.2007.11.005
11. Paton, C., Hellstrom, J., Paul, B., Woodhead, J. & Hergt, J. (2011). Iolite: freeware for the visualisation and processing of mass spectrometric data. J. Anal. At. Spectrom., 26, pp. 2508-2518. https://doi.org/10.1039/C1JA10172B
12. Artemenko, G. V. & Shumlyanskyy, L. V. (2021). The Paleoarchean (3,3 Ga) and Mesoarchean (3,0 Ga) tonalite-trondhjemite-granodiorite rocks of the West Azov Area (the Ukrainian Shield). Geologìčnij žurnal, No. 3, pp. 35-47. https://doi.org/10.30836/igs.1025-6814.2021.3.228873
13. Artemenko, G. V., Shumlyanskyy, L. V. & Shvaika, I. A. (2014). The late Paleoarchean tonalite gneisses of West-Azov block (Azov megablock of Ukrainian shield). Geologičnij žurnal, No. 4, pp. 91-102 (in Russian). https://doi.org/10.30836/igs.1025-6814.2014.4.139191
14. Artemenko, G. V., Shumlyanskyy, L. V., Wilde, S. A., Whitehouse, M. J. & Bekker, A. Yu. (2021). The U-Pb age and Lu-Hf isotope systematics of zircon from the Huliaipole metavolcanics, the Azov domain of the Ukrainian shield: evidence for the Paleoarchean-Hadean crust. Geologičnij žurnal, No. 1, pp. 3-16. https://doi.org/10.30836/igs.1025-6814.2021.1.216989
15. Bibikova, E. V. & Williams, I. S. (1990). Ion microprobe U-Th-Pb isotopic studies of zircons from three early Precambrian areas in the U.S.S.R. Precambrian Res., 48, pp. 203-221. https://doi.org/10.1016/0301-9268(90)90009-F
16. Lobach-Zhuchenko, S. B., Bibikova, E. V., Balagansky, V. A., Sergeev, S. A., Artemenko, G. V., Arestova, N. A., Shcherbak, N. P., Presnyakov, S. L. (2010). Paleoarchean tonalites in the Paleoproterozoic Orekhiv-Pavlohrad collision zone of the Ukrainian Shield. Doklady AN, 433, No. 2, P. 212-218 (in Russian).
17. Shcherbak, N. P., Artemenko, G. V. Lesnaya, I. M. & Ponomarenko, A. N. (2005). Geochronology of the Early Precambrian of the Ukrainian Shield (Archaean). Kyiv: Naukova Dumka (in Russian).
18. Bibikova, E. V., Claesson, S., Fedotova, A. A., Artemenko, G. V. & Ilyinsky, L. (2010). Terrigenous zircon of the Archean greenstone belts — a source of information about the early crust of the Earth: Azov and Dnieper regions, Ukrainian Shield. Geokhimiya, No. 9, pp. 899-916 (in Russian).

19. Bibikova, E., Fedotova, A., Claesson, S., Anosova, M. & Shumlyanskyy, L. (2013). The time of the continental crust origin in the early history of the Earth: isotopic and geochemical (U-Th-Pb, Lu-Hf, REE) study of terrigenous zircons of Archean metasedimentary rocks Sarmatia. In Problems of the Origin and Evolution of the Biosphere (pp. 147-167). Moscow: Krasand (in Russian).
20. Savko, K. A., Samsonov, A. V., Chervyakovskaya, M. V., Korish, E. Kh., Larionov, A. N. & Bazikov, N. S. (2020). Age and Lu-Hf isotope systematics of zircon from metapelite granulites of the Kursk-Besedino Domain: evidence of the Paleoarchean crust within the Kursk Block of Sarmatia. Vestnik VGU, Ser. Geologia, 2020, No. 3, pp. 30-44 (in Russian). https://doi.org/10.17308/geology.2020.3/3007
21. Savko, K. A., Samsonov, A. V., Larionov, A. N., Chervyakovskaya, M. V., Korish, E. H., Larionova, Y. O., Bazikov, N. S. & Tsybulyaev, S. V. (2021). A buried Paleoarchean core of the Eastern Sarmatia, Kursk block: U-Pb, Lu-Hf and Sm-Nd isotope mapping and paleotectonic application. Precambrian Res., 353, 106021. https://doi.org/10.1016/j.precamres.2020.106021
22. Artemenko, G. V., Shumlyanskyy, L. V., Bekker, A. Yu. & Hoffmann, A. (2022). Zircon age of metarhyodacite of the Aleksandrovsk suite of the Mykhailivka series (megablock KMA). Geochemistry and ore formation, Iss. 43, pp. 3-11 (in Ukrainian). https://doi.org/10.15407/gof.2022.43.003
23. Savko, K. A., Samsonov, A. V., Larionov, A. N., Korish, E. H., Chervyakovskaya, M. V. & Bazikov, N. S. (2019). Episodes of growth of the continental crust in the Early Precambrian of Sarmatia. In Fundamental problems of tectonics and geodynamics (Vol. 2), Materials of the LI Tectonic Meeting (pp. 270-273). Moscow: GEOS (in Russian).
24. Kröner, A. (2007). Chapter 5.2. The ancient gneiss complex of Swaziland and environs: record of early Archean crustal evolution in Southern Africa. In Earth's Oldest Rocks. Developments in Precambrian Geology (Vol. 15) (pp. 465-480). Elsevier. https://doi.org/10.1016/S0166-2635(07)15052-0
25. Ghosh, J. G. (2004). 3.56 Ga tonalite in the central part of the Bastar Craton, India: oldest Indian date. J. Asian Earth Sci., 23, pp. 359-364. https://doi.org/10.1016/S1367-9120(03)00136-6
26. Rajesh, H. M., Mukhopadhyay, J., Beukes, N. J., Belyanini, G. A. & Armstrong, R. A. (2009). Evidence for an early Archaean granite from Bastar Craton, India. J. Geol. Soc., 166, pp. 193-196. https://doi.org/10.1144/0016-76492008-089
27. Wan, Y.-S., Liu, D.-Y., Dong, C.-Y., Xie, H.-Q., Kröner, A., Ma, M.-Z., Liu, S.-J., Xie, S.-W. & Ren, P. (2015). Formation and Evolution of Archean Continental Crust of the North China Craton. In Precambrian Geology of China (pp. 59-136). Berlin, Heidelberg: Springer. https://doi.org/10.1007/978-3-662-47885-1_2
28. Iizuka, T., Komiya, T., Ueno, Y., Katayama, I., Uehara, Y., Maruyama, S., Hirata, T., Johnson, S. P. & Dunkley, D. J. (2007). Geology and zircon geochronology of the Acasta Gneiss Complex, northwestern Canada: new constraints on its tectonothermal history. Precambrian Res., 153, pp. 179-208. https://doi.org/10.1016/j.precamres.2006.11.017
29. Iizuka, T., Komiya, T., Johnson, S. P., Kon, Y., Maruyama, S. & Hirata, T. (2009). Reworking of Hadean crust in the Acasta gneisses, northwestern Canada: evidence from in-situ Lu–Hf isotope analysis of zircon. Chem. Geol., 259, pp. 230-239. https://doi.org/10.1016/j.chemgeo.2008.11.007

Received 01.05.2023

Г.В.Артеменко[1], https://orcid.org/0000-0002-4528-6853
Л.В. Шумлянський[1,2], https://orcid.org/0000-0002-6775-4419
Л.С. Довбиш[1]

[1] Інститут геохімії, мінералогії та рудоутворення ім. М.П. Семененка НАН України, Київ

[2] Кертінський університет, Школа наук про Землю та планети, Перт, Австралія

E-mail: regulgeo@gmail.com, leonid.shumlyanskyy@curtin.edu.au

ВІК ДЕТРИТОВОГО ЦИРКОНУ З МЕТАОСАДОВИХ ПОРІД ТЕРНУВАТСЬКОЇ ТОВЩІ (ЗАХІДНОПРИАЗОВСЬКИЙ БЛОК УЩ)

Тернуватська товща метаморфічних порід складає Гайчурську структуру дугоподібної форми завдовжки близько 72 км. Її західна частина знаходиться в зоні Андріївського розлому, який розділяє Вовчанський та Гуляйпільський блоки, а східна — у зоні Тернуватського розлому на Ремівському блоці. Породи, що формують Гайчурську структуру, характеризуються строкатим та мінливим по латералі складом та змінною потужністю, в них спостерігаються динамоструктури — розлінзування та розсланцювання. Верхня світа тернуватської товщі складена переважно метаосадовими породами — гнейсами та сланцями біотитовими, гранат-біотитовими, глиноземистими, магнетит-амфіболовими та польовошпатовими кварцитами. Нижня світа представлена вулканогенними породами — амфіболітами, метаультрабазитами та гнейсами біотит-амфіболовими. Методом LA-ICP-MS було продатовано 38 кристалів циркону з мусковіт-біотитових гнейсів верхньої світи тернуватської товщі, які за петрохімічними даними відповідають метаморфізованим граувакам. Серед них виявлено три популяції циркону — 3,65—3,45; 3,3 і 3,2—2,95 млрд років, які відповідають трьом етапам формування архейської кори Західноприазовського домену: утворенню найдавнішого фундаменту та граніт-зеленокам'яних комплексів палеоархейського і мезоархейського віку. Згідно з результатами зіставлення породних асоціацій Українського щита та Курської магнітної аномалії, очевидна відповідність палеоархейської кори (3,45—3,65 млрд років) Західноприазовського блока і Курсько-Бесединської грануліт-гнейсової області, а палеоархей-мезоархейські комплекси (2,9—3,3 млрд років) відповідають Михайлівській і Орловсько-Тимській структурам граніт-зеленокам'яної області Курської магнітної аномалії. Архейські комплекси Сарматського континенту є одновіковими з подібними утвореннями кратону Каапвааль у Південній Африці, Бастар в Індії, Північно-Китайського кратону, кратону Слейв у Канаді та інших, що формувалися починаючи з еоархею.

Ключові слова: *Гайчурська структура, тернуватська товща, мусковіт-біотитовий гнейс, Гуляйпільський блок, Вовчанський блок, Ремівський блок, циркон, U-Pb вік, метаосадові породи.*